ISSN 1070-3632, Russian Journal of General Chemistry, 2021, Vol. 91, No. 11, pp. 2167–2175. © Pleiades Publishing, Ltd., 2021.
Russian Text © The Author(s), 2021, published in Zhurnal Obshchei Khimii, 2021, Vol. 91, No. 11, pp. 1693–1703.

Synthesis and Properties of Iron(II) and Copper(II) Coordination Compounds with 2,6-Bis[1-(phenylimino)ethyl]pyridine

L. G. Lavrenova[a,*], A. A. Mishchenko[a,b], I. V. Oleynik[c], E. V. Korotaev[a], A. N. Lavrov[a], M. A. Grebenkina[a,b], L. A. Sheludyakova[a], L. S. Klyushova[d], and I. I. Oleynik[c]

[a] *A.V. Nikolaev Institute of Inorganic Chemistry, Siberian Branch of the Russian Academy of Sciences, Novosibirsk, 630090 Russia*
[b] *Novosibirsk National Research State University, Novosibirsk, 630090 Russia*
[c] *N.N. Vorozhtsov Novosibirsk Institute of Organic Chemistry, Siberian Branch of the Russian Academy of Sciences, Novosibirsk, 630090 Russia*
[d] *Institute of Molecular Biology and Biophysics, Federal Research Center for Fundamental and Translational Medicine, Novosibirsk, 630117 Russia*
**e-mail: ludm@niic.nsc.ru*

Received August 12, 2021; revised September 1, 2021; accepted September 5, 2021

Abstract—New iron(II) and copper(II) coordination compounds with 2,6-bis[1-(phenylimino)ethyl]pyridine (L^1), $Fe(L^1)_2SO_4 \cdot H_2O$, $Fe(L^1)_2(ClO_4)_2$, $Cu(L^1)Cl_2$, and $Cu(L^1)_2Br_2 \cdot 2H_2O$, were synthesized. The compounds were identified and investigated using CHN analysis and electronic spectroscopy (diffuse reflectance spectroscopy), IR spectroscopy, XRD, and static magnetic susceptibility. Antiferromagnetic exchange interactions between paramagnetic centers are observed in all iron and copper complexes in the ranges 80–420 and 1.77–300 K, respectively. Evaluation of the cytotoxic activity of copper(II) complexes showed that the $Cu(L^1)_2Br_2$ complex (IC_{50} 26.7 μmol/L) exhibits the highest activity against the human breast adenocarcinoma cell line (MCF-7).

Keywords: complexes, iron(II), copper(II), 2,6-bis[1-(phenylimino)ethyl]pyridine, magnetic and cytotoxic activity

DOI: 10.1134/S1070363221110062

Polynitrogen-containing heterocyclic compounds are a promising class of ligands for the synthesis of transition metal coordination compounds with magnetic, biological, and catalytic activity. Bisiminopyridine complexes are capable of catalyzing the ethylene polymerization to linear polyethylene [1–3], the reactions of [2+2] cycloaddition of unactivated olefins [4], the C–H functionalization [5], the hydroboration and hydrosilylation of alkenes [6, 7], and the activation of small molecules (N_2, O_2, CO_2) [8–10]. In bisiminopyridine complexes of metals with electronic configurations d^4–d^7, a spin crossover (spin transition) can take place under specific conditions. The change in the spin multiplicity occurs under the influence of temperature, pressure, irradiation with light of a certain wavelength, and other factors. This class of complexes includes iron(II) compounds with nitrogen-containing ligands, in which the spin transition $^1A_1 \leftrightarrow {}^5T_2$ is observed [11–13]. In Co(II), Ni(II), and Cu(II) polynuclear complexes with ligands of this class, antiferro- or ferromagnetic exchange interactions between paramagnetic centers are observed. A necessary condition for their occurring is cooperative interactions in the solid phase of the complexes [14]. The search for new molecular magnets is an important task of modern chemistry.

Potential nitrogen-containing ligands include pyridine derivatives—2,6-bis[1-(phenylimino)ethyl]pyridine (L^1) and 2,6-bis(benzimidazol-2-yl)pyridine (L^2, Scheme 1), which have the structure, which predetermines their tridentate cyclic mode of coordination to a central ion on complex formation. The coordination of two such ligands to a metal, in particular to Fe(II), leads to the formation of an octahedral polyhedron with a

Scheme 1.

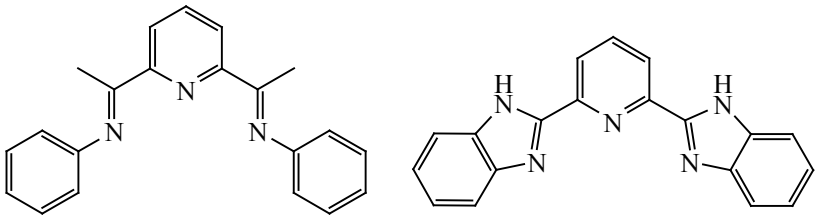

L^1 L^2

coordination node FeN_6, which is a prerequisite for the spin crossover occurrence. We have previously synthesized iron(II) complexes $[Fe(L^2)_2]A_i \cdot nH_2O$ (A is an anion; i = 1, 2; n = 0–2), with the compound L^2 and various anions in which the spin crossover $^1A_1 \leftrightarrow {}^5T_2$ is observed [15–17]. It seemed ppropriate to continue studies with this class of ligands, in particular, with the compound L^1. This ligand previously served as the basis for the synthesis of a number of compounds with double- and triple-charged 3*d* metal ions and Cd(II) [18–26]. Most of the synthesized complexes have the composition $[M(L^1)A_i]$ (i = 2, 3). The ligand is coordinated to the metal in a tridentate-cyclic type by three nitrogen atoms, the coordination nodes are supplemented up to five by halide ions (Cl^-, Br^-) or oxygen atoms of the nitrate ion [26, 27]. Complexes with two L^1 ligands, $[Ni(L^1)_2](BF_4)_2$ [26] and $[Cu(L^1)_2](ClO_4)_2$ [27], were obtained. Most complexes with the L^1 ligand exhibit catalytic and luminescent properties; their magnetic and biological activity has not been studied.

We synthesized Fe(II) and Cu(II) complexes with the ligand L^1, $Fe(L^1)_2SO_4 \cdot H_2O$, $Fe(L^1)_2(ClO_4)_2$, $Cu(L^1)Cl_2$, and $Cu(L^1)_2Br_2 \cdot 2H_2O$, and investigated their magnetic and cytotoxic properties. Complexes $Fe(L^1)_2SO_4 \cdot H_2O$ (**1**), $Fe(L^1)_2(ClO_4)_2$ (**2**), and $Cu(L^1)_2Br_2 \cdot 2H_2O$ (**4**) were isolated from aqueous-organic solutions at the stoichiometric ratio M : L^1 = 1 : 2. For the synthesis of complex $[Cu(L^1)Cl_2]$ (**3**) under the same conditions, the ratio M : L^1 = 1:2 was also used, however, a complex with the ratio M : L^1 = 1 : 1 was obtained. When synthesizing Fe(II) complexes, to preserve iron in the lowest oxidation state, ascorbic acid was added to solutions as a reducing agent and a weak acidifying reagent. The compound $[Fe(L^1)_2](ClO_4)_2$ was synthesized in two stages. At the first stage, a $Fe(ClO_4)_2$ solution was obtained by merging aqueous solutions of $FeSO_4$ and $Ba(ClO_4)_2$; at the second stage, a reaction between the $Fe(ClO_4)_2$ and L^1 solutions occurred. The resulting complexes are stable when stored in air and decompose without melting when heated to 450 K.

The $Cu(L^1)Cl_2$ complex was obtained earlier [26]. According to X-ray diffraction data, ligand L^1 in this complex is coordinated to Cu(II) by three nitrogen atoms, the structure of the coordination polyhedron is complemented to bipyramidal by two chloride ions to form the CuN_3Cl_2 node. The same way of L^1 coordination was found in the above-mentioned complexes with two L^1 ligands: $[Cu(L^1)_2](ClO_4)_2$ [26] and $[Ni(L^1)_2](BF_4)_2$ [27]. These compounds have a distorted octahedral structure of the coordination polyhedron with the MN_6 node; the anions occupy the outer-sphere position.

The main vibrational frequencies in the IR spectra of the compound L^1 and complexes are given in Table 1. In the range 3200–3050 cm^{-1} there are stretching vibrations of NH groups, in the range 3100–2850 cm^{-1}—stretching vibrations ν(CH) and ν(CH_3), and in the range 1650–1450 cm^{-1}—stretching and bending vibrations of benzene and pyridine cycles. In the spectra of the complexes in the range of ring vibrations, the number and position of bands differ from those in the spectrum of compound L^1, which points to the coordination of nitrogen atoms of pyridine and imino groups to the metal ions. This conclusion is confirmed by the spectra in the far-region, where the bands of metal–ligand vibrations appear, which are absent in the compound L^1 spectrum. This range contains bands that can be attributed to the ν(M–N) and ν(M–Cl) vibrations (Table 1).

The magnetic susceptibility $\chi_p(T)$ of the $CuLCl_2$ complex points to its paramagnetism and in the temperature range 50–300 K can be formally described by the Curie–Weiss dependence with the effective moment $\mu_{eff} \approx 1.83\ \mu_B$ and $\theta \approx -5$ K (Fig. 1). However, when the interval of data processing is shifted towards

Table 1. Main vibrational frequencies (cm^{-1}) in the spectra of the L^1 ligand and $[M(L^1)_2]A_2$ complexes

Assignment	L^1	$[Fe(L^1)_2SO_4]\cdot H_2O$	$[Fe(L^1)_2](ClO_4)_2$	$[Cu(L^1)Cl_2]$	$[Cu(L^1)_2]Br_2\cdot 2H_2O$
ν(CH)	3069	3059	3095	3064	3069
	3054		3078	3033	3036
	3044				
	3029				
$\nu(CH_3)$	2969	2954	2967	2948	2949
	2923	2922	2921	2908	2906
	2855	2852	2854	2855	2855
Ring vibrations + ν(C=N)	1636	1692	1691	1617	1614
	1591	1665	1588	1582	1579
	1572	1589	1560		1482
	1481	1524	1527		
		1481			
ν(M–N)		253 226	240	213	227
ν(Cu–Cl)				286	

low temperatures, the value of θ decreases by a factor of more than 20, and the dependence $\chi_p(T)$ shows no signs of antiferromagnetic ordering up to 1.77 K. This indicates that the real antiferromagnetic exchange interaction between copper ions is much weaker than would be expected from the value of θ obtained at high temperatures. The picture is clarified by the temperature dependence of the effective moment μ_{eff} calculated for θ equal to zero (Fig. 1). The value of μ_{eff} at 300 K is close to the theoretical value of 1.73 μ_B for spin-only (S = 1/2) moments of Cu^{2+} ions; the slight excess is due to the contribution of the orbital angular moments. As the

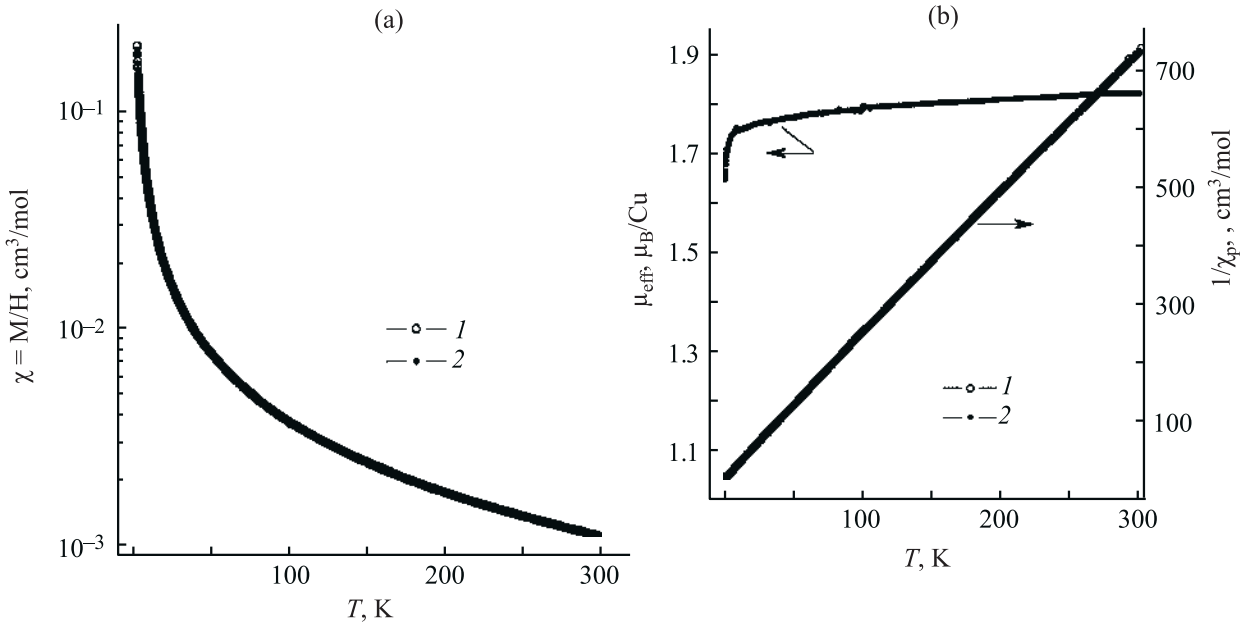

Fig. 1. (a) Temperature dependence of the magnetic susceptibility χ for the $CuLCl_2$ complex measured in the magnetic field H of (*1*) 1 and (*2*) 10 kOe, (b) the temperature dependence of the paramagnetic part of the susceptibility (in coordinates $1/\chi_p$) and the temperature dependence of the effective magnetic moment μ_{eff} calculated in the approximation of non-interacting moments (θ = 0).

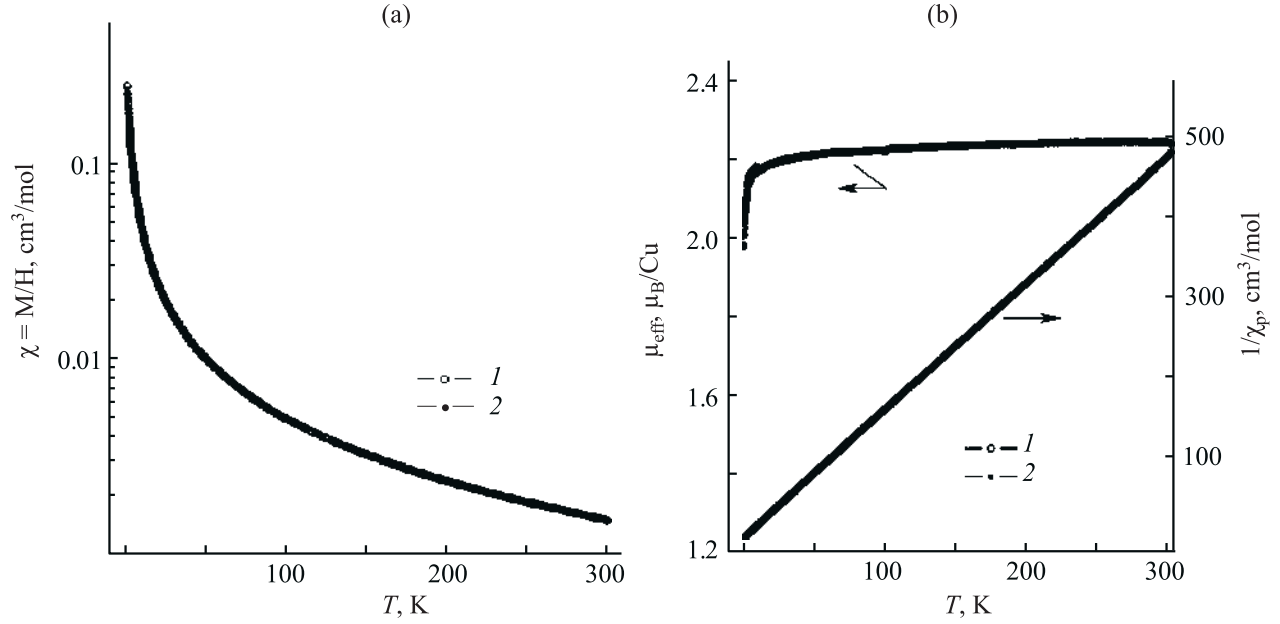

Fig. 2. (a) Temperature dependence of the magnetic susceptibility χ for the $CuL_2Br_2 \cdot 2H_2O$ complex measured in the magnetic field H of (*1*) 1 and (*2*) 10 kOe, (b) the temperature dependence of the paramagnetic part of the susceptibility (in coordinates $1/\chi_p$) and the temperature dependence of the effective magnetic moment μ_{eff} calculated in the approximation of non-interacting moments ($\theta = 0$).

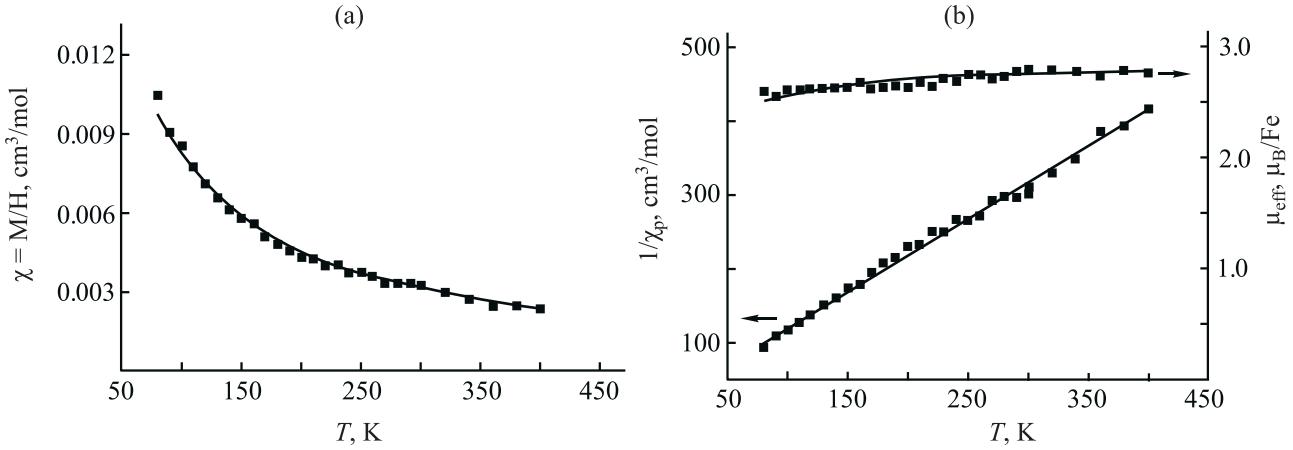

Fig. 3. (a) Temperature dependence of the magnetic susceptibility χ for the $Fe(L^1)_2SO_4$ complex (recording in an open ampoule); (b) $1/\chi$ and μ_{eff} calculated in the noninteracting spin approximation.

temperature decreases to ~ 10 K, μ_{eff} smoothly decreases, which may point to the "freezing out" of orbital angular moments with μ_{eff} tending to the spin-only value of 1.73 μ_B. A sharp decrease in μ_{eff} at the lowest temperatures (below 10 K) points to a weak antiferromagnetic interaction between Cu^{2+} ions.

For the $CuL_2Br_2 \cdot 2H_2O$ complex, the magnetic susceptibility $\chi_p(T)$ in the temperature range 20–300 K is well described by the Curie–Weiss law, $\mu_{eff} \approx 2.24\ \mu_B$ and $\theta \approx -1$ K (Fig. 2). The resulting effective moment significantly exceeds the theoretical value of 1.73 μ_B for spin-only (S = 1/2) moments of Cu^{2+} ions and points to a large contribution of orbital moments. The decrease in μ_{eff} observed at the lowest temperatures (<10 K) points to a weak antiferromagnetic interaction of the copper moments.

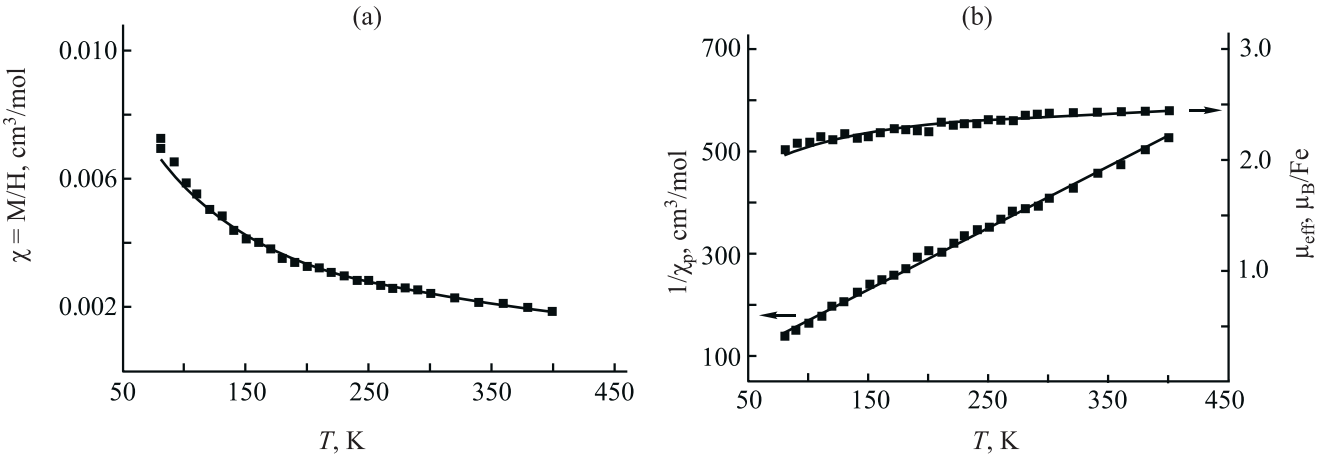

Fig. 4. (a) Temperature dependence of the magnetic susceptibility χ for the $[Fe(L^1)_2]SO_4 \cdot H_2O$ complex (recording in a sealed ampoule); (b) $1/\chi$ and μ_{eff} calculated in the noninteracting spin approximation.

The temperature dependences of the magnetic susceptibility of the $Fe(L^1)_2SO_4 \cdot H_2O$ complex were studied in the range of 80-400 K (Figs. 3 and 4). At ~420 K, the compound decomposes. Spin crossover is not observed regardless of the presence or absence of crystallization water in the compound.

The negative sign of θ for the dehydrated complex (–25 ± 3 K) and for the crystallohydrate (–47 ± 3 K) points to the antiferromagnetic interaction between iron magnetic moments in the substance. The values of the effective magnetic moment calculated in the noninteracting spin approximation (θ 0, Figs. 3 and 4) lie in the ranges of ~2.5–2.7 and ~2.1–2.4 μ_B. The values corresponding to these ranges, μ_{eff} 2.87 ± 0.03 μ_B for $[FeL_2]SO_4$ and μ_{eff} 2.59±0.03 μ_B for $[FeL_2]SO_4 \cdot H_2O$ obtained with regard to θ, are less than the theoretical "spin-only" value of 4.9 μ_B for Fe(II). If we assume that the compound contains iron(II) ions both in the high-spin (HS) and low-spin (LS) states, then based on the μ_{eff} values obtained with regard to θ, we can estimate the ratio HS : LS = 0.34 : 0.66 for dehydrated complex and HS : LS = 0.28 : 0.72 for the crystallohydrate. Thus, dehydration of the complex is accompanied by an increase in μ_{eff} and a weakening of antiferromagnetic interactions.

Negative values of the static magnetic susceptibility of the $Fe(L^1)_2(ClO_4)_2$ complex are observed in the temperature range up to 420 K. With a further increase in temperature, intense decomposition of the compound begins. Thus, the Fe(II) ions in the studied compound are in the low-spin state, μ_{eff} 0, and the compound itself is diamagnetic both in the presence of water of crystallization and in the dehydrated state (Fig. 5).

The XRD data showed that all the obtained complexes are crystalline; however we failed to grow their single crystals. Based on indirect methods and comparison with published data, it can be concluded that compound L^1 in the synthesized complexes with two ligands is coordinated in the same way as in the $[Cu(L^1)_2](ClO_4)_2$ [26] and $[Ni(L^1)_2](BF_4)_2$ [27] complexes with the formation of a distorted octahedral coordination polyhedron and the node MN_6 (M = Fe, Cu). This is confirmed by the character of the diffuse reflectance spectra. In the diffuse reflectance spectra of $Fe(L^1)_2SO_4 \cdot H_2O$, the bands at 485 and 745 nm can be attributed to *d–d* transitions $^1A_1 \rightarrow {}^1T_1$ (20619 cm^{-1}) and $^5T_2 \rightarrow {}^5E$ (13423 cm^{-1}) in distorted octahedral iron(II) complexes with the coordination node FeN_6 [28]. Consequently, the complex contains both the low-spin $^1A_1$ form and the high-spin $^5T_2$ form in the ratio calculated from the magnetochemical data. In the diffuse reflectance spectra of $Fe(L^1)_2(ClO_4)_2$, the only band at 744 nm corresponds to the *d–d* transition $^5T_2 \rightarrow {}^5E$ (13440 cm^{-1}), which points to the high-spin state of the complex.

The effect of copper(II) complexes on the viability of HepG2 and MCF-7 human cells was assessed in the presence of the test compounds dissolved in ethanol by the method of double staining with Hoechst 33342/PI followed by differentiation of cells into living, dead,

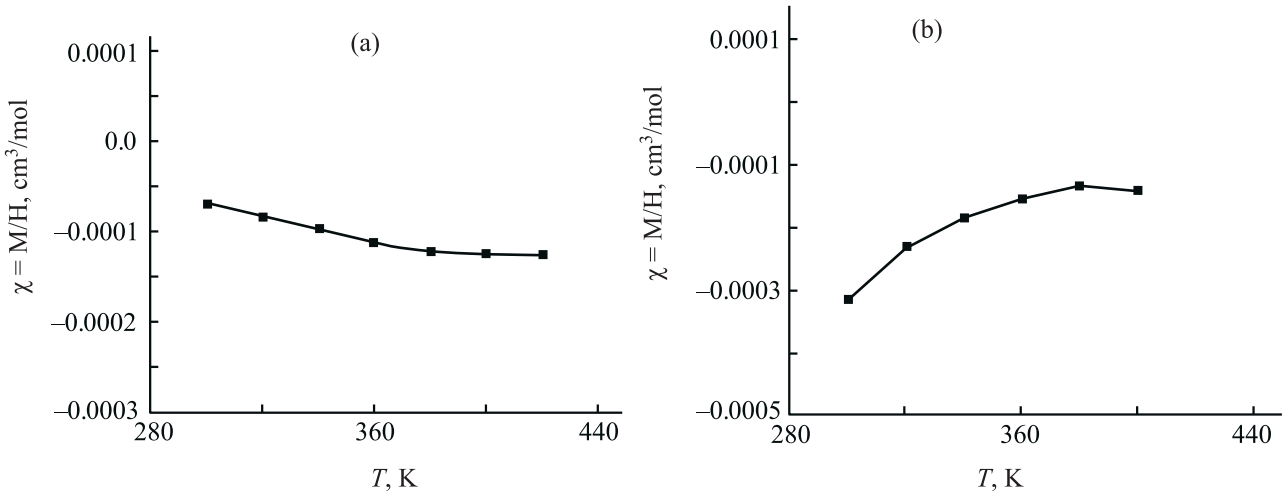

Fig. 5. Temperature dependences of the magnetic susceptibility χ for the $Fe(L^1)_2(ClO_4)_2$ complex. Recording in (a) an open ampoule and (b) a sealed ampoule.

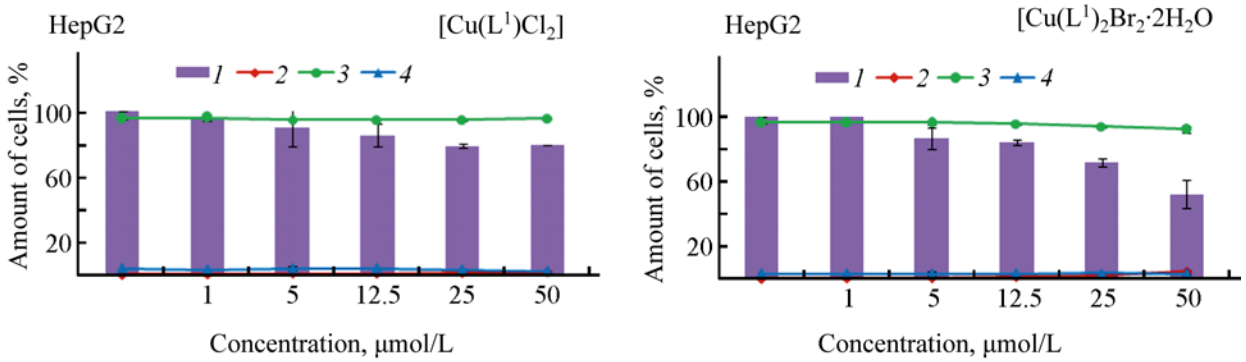

Fig. 6. Influence of complexes of copper(II) halides with 2,6-bis[1-(phenylimino) ethyl]pyridine on the viability of HepG2 cells. (*1*) Amount of cells, (*2*) dead cells, (*3*) living cells, and (*4*) apoptosis.

and apoptotic. Semi-maximal inhibition (IC_{50}), i.e. the concentration of the drug at which cell death is 50%, was calculated after nonlinear approximation of the curves of experimental dependence of cell survival on the substance concentration.

Copper(II) complexes showed no cytotoxic activity against the HepG2 cell line (Fig. 6), but exerted a cytostatic effect. The action of the $[CuL^1Cl_2]$ complex, starting from its concentration of 25 μmol/L, led to a slight decrease in the rate of cell growth, whereas the action of the 50 μmol/L $[Cu(L^1)_2]Br_2{\cdot}2H_2O$ solution twice reduced it in comparison with a control. The MCF-7 cell line was found to be more sensitive to the effects of the complexes under study (Fig. 7). The action of a 25 μmol/L solution of copper(II) bromide with L^1 on the MCF-7 cell line caused the death of ~50% of cells (IC_{50} 26.7 ± 0.5 μmol/L), whereas the maximal experimental concentration of copper (II) chloride with L^1 caused the death of ~10% of cells. Thus, in relation to the both cell lines, copper(II) bromide had a more active effect on cell viability as compared to copper(II) chloride.

EXPERIMENTAL

Commercial metal salts and solvents were used in the synthesis without further purification.

The IR absorption spectra of the complexes were recorded on Scimitar FTS 2000 and Vertex 80 IR

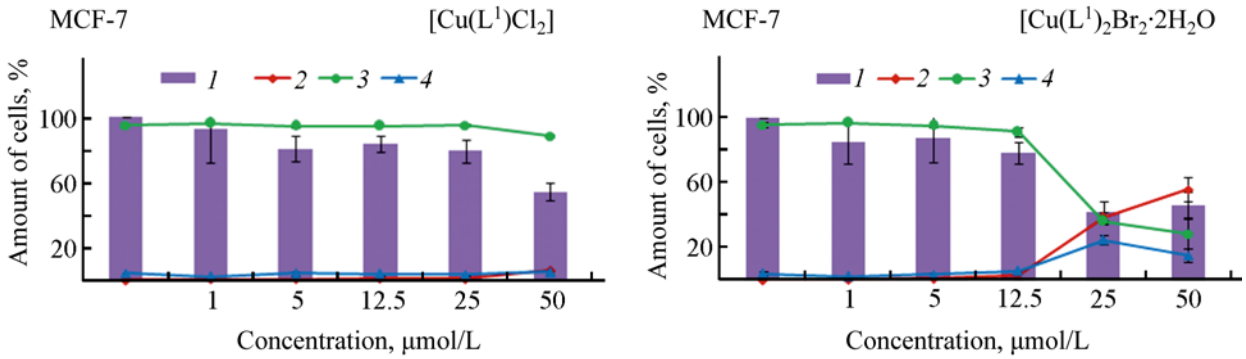

Fig. 7. Influence of complexes of copper(II) halides with 2,6-bis [1-(phenylimino)ethyl]pyridine on the viability of MCF-7 cells. (*1*) Amount of cells, (*2*) dead cells, (*3*) living cells, and (*4*) apoptosis.

Fourier spectrometers in the ranges 4000–400 cm^{-1} and 400–100 cm^{-1}, respectively. The samples were prepared in the form of suspensions in Vaseline and fluorinated oils and in polyethylene. The diffuse reflectance spectra were recorded on a UV-3101 PC Shimadzu scanning spectrophotometer at room temperature in the range 300–2000 nm. The ^1H NMR spectra were recorded on a Bruker AV-400 instrument with an operating frequency of 400.13 MHz.

The static magnetic susceptibility of copper complexes was measured on a Quantum Design MPMS-XL SQUID magnetometer in the temperature range 1.77–300 K and magnetic field H range 0–10 kOe. Magnetic properties of the iron complexes were studied by the Faraday method in the temperature range 80–420 K at H 0–7.3 kOe. To study the dehydrated iron complexes, the samples were placed in open quartz ampoules and evacuated to a residual pressure of 10^{-2} mmHg in the measuring cell of the installation, then an inert atmosphere of helium at a pressure of 5 mmHg was created. When studying iron complexes containing crystallization water, the samples were sealed in quartz ampoules with atmospheric air.

The temperature-independent contribution χ_d was calculated using the Pascal additive scheme. To determine the effective magnetic moment of copper and iron ions μ_{eff} and the Weiss constant θ, the temperature dependences of the paramagnetic contribution to the magnetic susceptibility $\chi_p(T) = \chi(T)–\chi_d$ were analyzed using the Curie–Weiss dependence (1).

$$\chi_p(T) = N_A\mu_{eff}^2/3k_B(T-\theta). \quad (1)$$

Here N_A and k_B are Avogadro's number and Boltzmann's constant, respectively ($\mu_{eff} = [(3k_B/N_A)\chi_p(T-\theta)]^{1/2}$). The values of the Weiss constant θ obtained in the processing made it possible to estimate the exchange interaction parameters.

Biological research was performed on human cell lines HepG2 (hepatocellular carcinoma) and MCF-7 (breast adenocarcinoma). Cell viability was evaluated by the method of double staining with Hoechst 33342/propidium iodide (PI) according to the standard method described earlier [29]. The cells were seeded on 96-well plates and cultured in the IMDM medium (Sigma-Aldrich, USA) supplemented with 10% fetal bovine serum (HyClone, Germany) in a CO_2 incubator at 37°C. After 24 h, preparations dissolved in EtOH were added in the concentration range of 1–50 μmol/L and incubated for 48 h. The cells were stained with Hoechst 33342 fluorescent dyes (Sigma-Aldrich) and propidium iodide (Invitrogen) for 30 min at 37°C. The survey was performed on an IN Cell Analyzer 2200 (GE Healthcare, UK) in an automatic mode, 4 fields per well. Images were processed using In Cell Investigator software to determine living (normal nuclei—blue non-condensed chromatin evenly distributed throughout the nucleus), dead (red, enlarged nuclei with smooth normal structure or bright red with slightly condensed chromatin), and apoptotic (round cells, bright blue strongly condensed or fragmented chromatin) cells in the entire population. The result is presented as the percentage of cells from three independent experiments ± standard deviation.

2,6-Bis[1-(phenylimino)ethyl]pyridine (L^1) was synthesized with 70% yield by refluxing 2,6-diacetylpyridine with an excess of aniline in methanol in the

presence of catalytic amounts of formic acid as described in [30]. ^{1}H NMR spectrum (400 MHz, $CDCl_3$), δ, ppm: 2.40 s (6H, Me), 6.84 d (4H_{Ar}, J 7.9 Hz), 7.11 t (2H_{Ar}, *J* 7.3 Hz), 7.37 t (4H_{Ar}, *J* 7.7 Hz), 7.86 t (1H, $H^4{}_{Py}$, *J* 7.8 Hz), 8.34 d (2H, $H^{3.5}{}_{Py}$, *J* 7.8 Hz).

$[Fe(L^1)_2]SO_4 \cdot H_2O$ (1). A weighed portion of 1 mmol (0.28 g) of $FeSO_4 \cdot 7H_2O$ with addition of 0.1 g of ascorbic acid was dissolved with heating in 10 mL of water, and 2 mmol (0.62 g) of L^1 was dissolved in 10 mL of methylene chloride, the solutions were heated and mixed. The resulting red solution was evaporated until a precipitate began to form. After cooling the solution with the precipitate in a crystallizer with ice, the red-violet precipitate was filtered off, washed two times with small portions of water, and dried in air. Yield 20%. Found, %: C 63.5; H 5.6; N 9.2. $C_{42}H_{40}FeN_6O_5S$. Calculated,%: C 63.3; H 5.1; N 10.5.

$[Fe(L^1)_2](ClO_4)_2$ (2). Weighed portions of 1 mmol (0.28 g) of $FeSO_4 \cdot 7H_2O$ and 1 mmol (0.34 g) of $Ba(ClO_4)_2$ with addition of 0.1 g of ascorbic acid were dissolved separately with heating in 10 mL of water each, then the resulting solutions were mixed. The $BaSO_4$ precipitate was filtered off, and a solution of 2 mmol (0.62 g) of L^1 in 10 mL of methylene chloride was added to the resulting solution of $Fe(ClO_4)_2$. The resulting red solution was evaporated until a precipitate began to form. After cooling the solution with the precipitate in a crystallizer with ice, the red-violet precipitate was filtered off, washed two times with small portions of methylene chloride, and dried in air. Yield 11%. Found, %: C 57.7; H 4.4; N 9.4. $C_{42}H_{38}Cl_2FeN_6O_8$. Calculated, %: C 57.2; H 4.3; N 9.5.

$[Cu(L^1)Cl_2]$ (3). A weighed portion of 1.5 mmol (0.27 g) of $CuCl_2$ was dissolved with heating in 5 mL of ethanol, and 3 mmol (0.93 g) of compound L^1—in 15 mL of methylene chloride; the solutions were mixed. To the resulting green solution, 10 mL of hexane was added. On cooling the solution, a green precipitate of the complex formed, which was washed two times with small portions of ethanol, and dried in air. Yield 55%. Found, %: C 55.9; H 4.3; N 9.2. $C_{21}H_{19}Cl_2CuN_3$. Calculated, %: C 56.3; H 4.3; N 9.4.

$[Cu(L^1)_2]Br_2 \cdot 2H_2O$ (4). Weighed portions of 0.5 mmol (0.11 g) of $CuBr_2$ and 1 mmol (0.31 g) of compound L^1 were dissolved with heating in 5 mL of ethanol and 10 mL of methylene chloride, respectively, and then the resulting solutions were mixed. The resulting brown solution was boiled to remove excess solvent. After cooling the solution in a crystallizer with ice, a brown precipitate formed, which was filtered off, washed two times with small portions of ethanol, and dried in air. Yield 48%. Found, %: C 56.5; H 4.5; N 9.6. $C_{42}H_{42}Br_2CuN_6O_2$. Calculated, %: C 56.9; H 4.8; N 9.5.

AUTHOR INFORMATION

L.G. Lavrenova, ORCID: https://orcid.org/0000-0003-4451-1630

I.V. Oleynik, ORCID: https://orcid.org/0000-0002-2686-3889

E.V. Korotaev, ORCID: https://orcid.org/0000-0001-7735-0285

A.N. Lavrov, ORCID: https://orcid.org/0000-0002-2436-017X

M.A. Grebenkina, ORCID: https://orcid.org/0000-0001-5604-2291

L.S. Klyushova, ORCID: https://orcid.org/0000-0003-4820-2536

I.I. Oleynik, ORCID: https://orcid.org/0000-0001-7232-6200

FUNDING

This work was supported by the Russian science foundation (grant no. 20-63-46026) and the Ministry of science and higher education of the Russian Federation (projects nos. 121031700313-8, 121031700314-5, and 121011490013-7). Experiments on the analysis of cytotoxicity were carried out using the equipment of the Center for collective use "Proteomic analysis" with the support of the Ministry of education and science of Russia (agreement no. 075-15-2021-691).

CONFLICT OF INTEREST

No conflict of interest was declared by the authors.

REFERENCES

1. Flisak, Z. and Sun, W.-H., *ACS Catal*., 2015, vol. 5, p. 4713. https://doi.org/10.1021/acscatal.5b00820
2. Gibson, V.C., Redshaw, C., and Solan, G.A., *Chem. Rev*., 2007, vol. 107, p. 1745. https://doi.org/10.1021/cr068437y
3. Oleinik, I.I., Oleinik, I.V., Abdrakhmanov, I.B., Ivanchev, S.S., and Tolstikov, G.A., *Russ. J. Gen. Chem*., 2004, vol. 74, no. 10, p. 1575. https://doi.org/10.1007/s11176-005-0059-7
4. Bouwkamp, M.W., Bowman, A.C., Lobkovsky, E.,

and Chirik, P.J., *J. Am. Chem. Soc*., 2006, vol. 128, p. 13340.
https://doi.org/10.1021/ja064711u

5. Tondreau, A.M., Stieber, S.C.E., Milsmann, C., Lobkovsky, E., Weyhermüller, T., Semproni, S.P., and Chirik, P.J., *Inorg. Chem*., 2013, vol. 52, p. 635.
https://doi.org/10.1021/ic301675t
6. Obligacion, J.V. and Chirik, P.J., *J. Am. Chem. Soc*., 2013, vol. 135, p. 19107.
https://doi.org/10.1021/ja4108148
7. Hojilla Atienza, C.C., Tondreau, A.M., Weller, K.J., Lewis, K.M., Cruse, R.W., Nye, S.A., Boyer, J.L., Delis, J.G.P., and Chirik, P.J., *ACS Catal*., 2012, vol. 2, p. 2169.
https://doi.org/10.1021/cs300584b
8. Margulieux, G.W., Turner, Z.R., and Chirik, P.J., *Angew. Chem. Int. Ed*., 2014, vol. 53, p. 14211.
https://doi.org/10.1002/anie.201408725
9. Badiei, Y.M., Siegler, M.A., and Goldberg, D.P., *J. Am. Chem. Soc*., 2011, vol. 133, p. 1274.
https://doi.org/10.1021/ja109923a
10. Rummelt, S.M., Zhong, H., Korobkov, I., and Chirik, P.J., *J. Am. Chem. Soc*., 2018, vol. 140, p. 11589.
https://doi.org/10.1021/jacs.8b07558
11. *Spin Crossover in Transition Metal Compounds, vols. I–III*, Gutlich, P. and Goodwin, H., Eds., Berlin: Springer, 2004, p. 233.
12. Halcrow, M.A., *Spin-Crossover Materials Properties and Applications*, Chichester: John Wiley & Sons Ltd, 2013.
13. Shakirova, O.G. and Lavrenova, L.G., *Crystals*, 2020, vol. 10, p. 843.
https://doi.org/10.3390/cryst10090843
14. Buchachenko, A.L., *Russ. Chem. Bull*., 2011, vol. 60, no. 12, p. 2439.
https://doi.org/10.1007/s11172-011-0378-2
15. Lavrenova, L.G., Dyukova, I.I., Korotaev, E.V., Sheludyakova, L.A., and Varnek, V.A., *Russ. J. Inorg. Chem*., 2020, vol. 65, no. 1, p. 30.
https://doi.org/10.1134/S0044457X20010109
16. Ivanova, A.D., Korotaev, E.V., Komarov, V.Yu., Sheludyakova, L.A., Varnek, V.A., and Lavrenova, L.G., *New J. Chem*., 2020, vol. 44, p. 5834.
https://doi.org/10.1039/d0nj00474
17. Ivanova, A.D., Lavrenova, L.G., Korotaev, E.V., Trubina, S.V., Sheludyakova, L.A., Petrov, S.A., Zhizhin, K.Yu., and Kuznetsov, N.T., *Russ. J. Inorg. Chem*., 2020, vol. 65, no. 11, p. 1687.
https://doi.org/10.31857/S0044457X20110070
18. Restivo, R.J. and Ferguson, G., *Dalton Trans*., 1976, p. 518.
19. Bluhm, M.E., Folli, C., and Döring, M., *J. Mol. Cat. A*, 2004, vol. 212, p. 13.
https://doi.org/10.1016/j.molcata.2003.11.003
20. Fan, R-Q., Zhu, D-S., Mu, Y., Guang-Hua, Li, G.-H., Yang, Y-L., Su, Q., and Feng, S.-H., *Eur. J. Inorg. Chem*., 2004, no. 24, p. 2304.
https://doi.org/10.1002/ejic.200400443
21. Gong, D., Baolin, Wang, B., Bai, C., Bi, J., Wang, F., Dong, W., Zhang, X., and Jiang, L., *Polymer*, 2009, vol. 50, p. 6259.
https://doi.org/10.1016/j.polymer.2009/10.054
22. Adnan, Abu-Surrah, Khalid, A.I., Maher, Y.A., and Ayman, A.I., *J. Polym. Res*., 2011, vol. 18, p. 59.
https://doi.org/10.1007/s10965-010-9391-7
23. Edwards, D.A., Mahon, M.F., Martin, W.R., Molloy, K.C., Fanwick, P.E., and Walton, R.A., *J. Chem. Soc. Dalton Trans*., 1990, p. 3161.
24. Guo, M.-P., Gui-Quan Guo, G.-Q., Guo, H.-R., and Di-Chang Zhong, D.-C., *Acta Crystallogr. E*, 2007, vol. 63, p. m3025.
https://doi.org/10.1107/S1600536807056644
25. Fan, R.-Q., Fan, R.-J., Lv, Z.-W., Lin Yang, Y.-L., An, F., and Gu, D.-M., *J. Coord. Chem*., 2007, vol. 60, no. 9, p. 919.
https://doi.org/10.1080/00958970600914267
26. Trivedi, M., Pandey, D.S., and Xu, Q., *Inorg. Chim. Acta*, 2007, vol. 360, p. 2492.
https://doi.org/10.1016/j.ica.2006.12.031
27. Blake, A.J., Lavery, A.J., Schröder, M., *Acta Crystallogr. C*, 1996, vol. 52, p. 37.
https://doi.org/10.1107/S0108270195009851
28. Lever, A.B.P., *Inorganic Electronic Spectroscopy*, Amsterdam: Elsevier, 1985.
29. Solovieva, A.O., Vorotnikov, Yu.A., Trifonova, K.E., Efremova, O.A., Krasilnikova, A.A., Brylev, K.A., Vorontsova, E.V., Avrorov, P.A., Shestopalova, L.V., Poveshchenko, A.F., Mironov, Yu.V., and Shestopalov, M.A., *J. Mater. Chem*. B, 2016, vol. 4, p. 4839.
https://doi.org/10.1039/C6TB00723F
30. Guo, J., Wang, B., Bi, J., Zhang, C., Zhang, H., Bai, C., Hu, Y., and Zhang, X., *Polymer*, 2015, vol. 59, p. 124.
https://doi.org/10.1016/j.polymer.2015.01.006